Density functional calculations of Ti-enhanced $NaAlH_4$

O. M. Løvvik
Center for Materials Science and Nanotechnology, University of Oslo, P. O.Box 1126, Blindern, NO-0318 Oslo, Norway

S. M. Opalka
United Technologies Research Center, 411 Silver Lane, East Hartford, Connecticut 06108, USA
(Received 13 September 2004; published 8 February 2005)

The crystal structure and thermodynamic stability of a number of proposed models for the inclusion of Ti in $NaAlH_4$ have been calculated by employing density functional theory in the generalized gradient approximation. It was shown that the least unfavorable location of Ti is close to the surface, replacing Al in the host lattice. Intricate complexation is simulated around the included Ti atom, and the preferred coordination number of H around Ti is eight. The Ti content was varied by the supercell approach, and even at 3 mol % Ti the resulting cell parameters were predicted to be significantly changed from the pure alanate. In addition, the most stable configurations were found to be thermodynamically metastable compared to the pure alanate and Ti standard state phases, and an ordered doped phase with significant bulk Ti content is thus ruled out by this study. It is proposed that Ti most probably works as a catalyst, situated at the surface of the alanate.

DOI: 10.1103/PhysRevB.71.054103 PACS number(s): 61.72.Ss, 71.20.Ps, 61.66.Fn

I. INTRODUCTION

One of the current lead candidates for a low cost and high hydrogen density, reversible hydrogen storage material is doped/catalyzed sodium alanate, $NaAlH_4$.[1–4] Of the numerous additives that have been investigated, it has been shown that titanium (Ti) is the additive that most efficiently increases the hydrogenation and dehydrogenation rates.[5] The cation radius of the additive was furthermore shown to correlate with its efficiency, while its valence did not seem to play a vital role.[5]

The role of the Ti additive is, however, still poorly understood. Ti may be added to the alanate in several different ways,[6] and so far one of the most successful ways of introduction is by using titanium nanoparticles as doping agents.[7,8] The high efficiency of the small Ti clusters is most easily explained by their very high dispersion, which makes their catalytic reactivity larger;[7,8] this lends support to the view that the role of Ti is primarily played at the surface.

Significant research efforts have been made both to identify the resulting Ti-bearing phase(s) that form when sodium alanate is ball-milled with a small weight fraction ($<$6 mol %) of a Ti inorganic salt or metal-organic compound, and to mechanistically investigate the resulting Ti catalysis of reversible sodium alanate hydrogenation/dehydrogenation reactions.[6,9–16] These studies have searched for evidence of whether Ti exists as a bulk dopant on the sodium alanate lattice, is adsorbed onto the surface akin to a metal-loaded heterogeneous catalyst, or is incorporated into another phase, such as an Al/Ti intermetallic compound. So far, only one published study has presented x-ray diffraction evidence of Ti incorporation as a bulk dopant, as changes in the sodium alanate lattice parameters with increasing additions of Ti-alkoxides.[11] The inconsistent changes reported over the range of 2–10 mol % Ti addition, were attributed to the saturation in Na vacancy formation and the resulting change in Ti charge/radius with increasing Ti dopant concentration. These results, however, have not been corroborated by other analyses. Both XANES,[14] synchrotron x-ray,[15] and Rietveld refinement of x-ray and neutron powder diffraction data[16] have found the sodium alanate lattice parameters to remain unchanged with the incorporation of Ti-additives. Ti has tentatively been identified to be present in an Al-Ti alloy,[6] on the surface in an amorphous $TiAl_3$ phase,[14] and solubilized in fcc Al upon dehydrogenation.[15] The latter study quantified the amount of Ti present in the Al sublattice to be around 30% of the total amount of added Ti.[15] These Ti-bearing phases may be difficult to confirm either due to their high dispersion and relatively small amount, or to their amorphous, x-ray indifferent structure. However, the related x-ray diffraction indications of a metastable $L1_2$ $TiAl_3$ phase in $NaAlH_4$ milled with 33 mol % $TiCl_3$,[17] and a stable $D0_{22}$ $TiAl_3$ phase in $LiAlH_4$ milled with 20 mol % $TiCl_4$ (Ref. 18) lends credibility to their possible existence.

The elemental distribution of Ti-doped $NaAlH_4$ after complete dehydrogenation has been investigated by scanning electron microscopy and energy dispersive spectroscopy, and Ti was primarily found in areas rich in Al.[10] This investigation was, however, performed on a sample doped by using a liquid alkoxide process, which shows poor cycling behavior.[19] $TiAl_3$ has been observed in a sample doped with $TiCl_3$,[17] but when $NaAlH_4$ was doped directly with $TiAl_3$, the kinetics were drastically lower than the $TiCl_3$ doped sample.[17]

In this paper, we turn to atomic scale modeling to gain insight as to whether it is favorable for Ti to be substituted as a dopant on the sodium alanate lattice. A recent density-functional simulation study has interpreted from predicted cohesive energies that Ti substitution on the sodium alanate lattice was more energetically favorable than the undoped phase, and preferentially occurred on the sodium sublattice without vacancy formation.[13] Here, we will report the incorporation of Ti into the sodium alanate lattice to be energetically unfavorable for any likely sublattice/vacancy combination at any Ti additive level, from 3 to 25 mol %. These results were from density-functional band-structure calculations, employing full relaxation of both the atomic positions and the cell size and shape. Thus, both effects of dopants on

the crystal structure, as well as the enthalpies of formation and substitution were calculated to clarify the stability of various models for adding Ti.

II. METHODOLOGY

The recent literature on the possible new Ti-bearing phases that may form upon blending Ti additives with $NaAlH_4$ does not provide enough structural and textural information to support their atomic simulation.[6,14,15] Therefore, our founding hypothesis is to indirectly assess the likelihood of their existence, by evaluating the feasibility of Ti substitution in the $NaAlH_4$ lattice. Indeed, if Ti-doping of $NaAlH_4$ is predicted to be energetically unfavorable, and/or if the simulated doped structures do not match recent experimental findings, the motivation for the theoretical identification and confirmation of the analytically proposed phases would be reinforced. Our focus is solely on the substituted $NaAlH_4$ lattice, and does not address the mechanism of the complete substitution reaction starting from the Ti additive and ending with the resulting by-product(s). Conceivably, substituted Ti ions could occupy Na or Al sublattice sites, or interstitial positions within the $NaAlH_4$ host. Both surface or bulk substitution scenarios are plausible, since it is envisioned that the Ti ion position would evolve with the moving phase front during the first-order sodium alanate dehydrogenation and reverse hydrogenation reactions/phase transformations. Following this rationale, we propose both bulk and surface substituted models for all possible site substitution combinations detailed in the forthcoming sections.

Ground state (0 K) periodic density functional theory (DFT) calculations with a plane-wave basis set were made with the Vienna *ab initio* simulation package (VASP)[20,21] using the generalized gradient approximation (GGA) of Perdew and Wang.[22] The projector augmented wave (PAW) method was used to span out the valence electron density.[23] The lowest energy structures were produced using the standard potentials with the valence configurations $3s^2\ 3p^1$ for Al and $1s^1$ for H, and the very hard potentials with the valence configurations $2s^2\ 2p^6\ 3s^1$ for Na, and $3s^2\ 3p^6\ 3d^2\ 4s^2$ for Ti. A cutoff energy of 780 eV and a Gaussian smearing method with an energy broadening of 0.2 eV was used throughout. The *k*-mesh generated with the Monkhorst-Pack method had a spacing of less than 0.5 $Å^{-1}$. For example, the 24 atom models with the starting equivalent of four $NaAlH_4$ groups were represented with eight *k* points or higher depending on the symmetry, and the 96 atom bulk and slab models with the starting equivalent of 16 $NaAlH_4$ groups were represented with one or higher, and eight *k* points, respectively. The criterion for self-consistency in the electronic structure determination was that two consecutive energies differed by less than 0.01 meV. The overall error due to the mentioned numerical sources was in the order of 1 meV per unit cell. The ground state energetics of the elements in their most stable standard state phase, $Im\bar{3}m$ Na metal, $Fm\bar{3}m$ Al metal, $P6_3/mmc$ Ti metal, and diatomic H_2 gas, supplied in the Materials Design MedeA software elemental thermodynamic database,[24] were used to determine the thermodynamic changes for $NaAlH_4$ doping reactions. These standard state elemental values were calculated with the same potentials, high precision, optimized odd-sized *k*-meshes with a *k*-point spacing of 0.2 $Å^{-1}$, and Bloechl corrections to the tetrahedron method were used to determine the thermodynamic changes for $NaAlH_4$ doping reactions. Theoretical vaules for the bulk lattice constants were used, and the cell used to simulate the H_2 gas was $1\times1\times1$ nm. The H_2 spin state was that of the experimental ground state, that is a singlet.

The previously calculated crystal structure of $NaAlH_4$,[25] which is very close to the experimentally determined one,[26] was used as basis for building periodic tetragonal cells and supercells of $NaAlH_4$ and its variations with possible Ti dopant configurations. Surface slab models were created by cleaving the doped lattices along the (001) crystallographic plane, the lowest energy $NaAlH_4$ low index surface identified in previous unpublished work.[27] The bulk relaxed values of the lattice parameters were used for all the slab calculations, allowing only the ionic coordinates to relax in those cases. The ionic coordinates of the bottom layer were kept constant, to mimic a bulk continuation of the slab in one direction. The vacuum region between periodic slabs was 1 nm. The surface energy of the slabs is converged at four metal layers,[27] and a four-layer $2\times2\times1$ 96 atom slab was used for most of the surface calculations.

The ground state (0 K) geometries of bulk and surface slab structures were determined by minimizing the Hellman-Feynman forces with the residual minimization method direct inversion in iterative subspace (RMM-DIIS) implementation of the quasi-Newton method. In the bulk models, full minimization of the atomic coordinates, cell size, and cell shape were conducted simultaneously. In the slab models, only the ionic positions were relaxed, keeping the bottom stoichiometric layer fixed to approximate bulk behavior. For both bulk and slab models, a series of calculations was made with increasing precision. The structure was said to be relaxed when all the forces of nonfixed atoms were less than 0.05 eV/Å. A single calculation using high accuracy was performed after the completion of the relaxation, to determine the accurate total energy. The VASP calculated total energies are actually the electronic energies with respect to the element atoms in a non-spin-polarized state. When these total energies are used in equations to determine heats of formation or reaction enthalpies, the uncorrected contributions from these artificial reference states are canceled.

III. TI AS BULK DOPANT

In order to efficiently span a wide range of possible site substitutions, we choose to first evaluate a 25 mol % Ti substitution per 1 mole $NaAlH_4$, in the conventional tetragonal cell containing a four $NaAlH_4$ formula unit (24 atom) basis. In practice, such a large substitution would not provide an advantage, the higher atomic weight Ti atoms would significantly decrease the gravimetric hydrogen storage capacity, and could result in significant $NaAlH_4$ decomposition from the initial metathesis reaction with the titanium additive.[17] However, higher Ti substitution levels enable more rapid simulations with smaller periodic bulk models, and also can provide important information for the thermodynamic as-

TABLE I. Results of the models for adding 25% Ti to the bulk $NaAlH_4$ crystal structure. The formal charge of Ti, Z_{Ti}, was assigned to be equal to the sum of the charges of the ions removed by direct titanium substitution and by concomitant vacancy formation, where the removed ions were assumed to have the following formal charges: $(Na)^{+1}$, $(Al)^{+3}$, and $(H)^{-1}$. The enthalpies of formation ΔH_{Form} and substitution ΔH_{Subst} are defined in Eqs. (1) and (2), and measure the stability of the different models relative to the elements and pure $NaAlH_4$, respectively. They are measured in kJ/mol atom. Ti is either put on the Na or Al sublattices, or in an interstitial (Int.) site described in the text. Also shown are the lattice constants measured in picometers (pm) and the angle (γ) that consistently showed the most change after relaxation of the lattice.

Model	Ti site	Substituted ions	Z_{Ti}	ΔH_{Form} (kJ/mol atom)	ΔH_{Subst} (kJ/mol atom)	a_{latt} (pm)	c_{latt} (pm)	γ (deg)
$4NaAlH_4$				−17.6		500	1111	90.00
$Na_4Ti(AlH_4)_4$	Int.	0	0	−10.9	6.0	498	1176	87.35
$Na_3Ti(AlH_4)_4$	Na	Na	+1	−8.0	9.5	472	1078	90.00
$Na_2Ti(AlH_4)_4$	Na	2 Na	+2	−6.4	11.9	455	1205	92.90
$NaTi(AlH_4)_4$	Na	3 Na	+3	−1.7	17.4	452	1018	90.00
$NaTi(AlH_4)_3$	Na	3 Na+AlH_4	+2	−9.5	15.3	482	1125	90.00
$Na_4(TiH_4)(AlH_4)_3$	Al	Al	+3	−14.2	3.4	491	1103	90.00
$Na_4(TiH_3)(AlH_4)_3$	Al	Al+H	+2	−14.7	3.6	487	1066	87.00
$Na_4(TiH_2)(AlH_4)_3$	Al	Al+H_2	+1	−6.1	13.1	526	1078	95.28
$Na_3(TiH_4)(AlH_4)_3$	Al	Al+Na	+4	−13.0	5.4	475	1121	90.00

sessment of solubility limits and lattice stabilities as a function of doping level. One important drawback for such small models is the artificial dopant interactions and superlattice formation that are apparent when the periodic models are extended in supercells.

Nine different possibilities for adding Ti in the bulk were considered, as shown in Table I in terms of the chemical formula, the substituted atoms, the formal charge of the Ti dopant, heats of formation, heats of substitution, and final relaxed structural parameters. The formal charges were merely used to book-keep different ionic configurations for proposing different starting models, and are generally not in agreement with charge densities approximated by integration of DFT results, using any ionic radius convention. In setting up the atomic models, all atomic potentials were prescribed using the full complement of valence electrons for the respective neutral atoms. The electron density is then redistributed to simulate the ionic/electronic interactions in the ground state minimum energy configuration during the VASP relaxations. Conceptually, the formal charge of the substituted Ti atom, Z_{Ti}, could range between 0 and +4, depending upon the substitution position and the creation of vacancies at other ion positions. The proposed bulk models sampled all the conceivable vacancy combinations that could represent this range of Ti formal charges. The first model simply added Ti as an absorbed species at the interstitial quasi-octahedral site surrounded by six H atoms at 175–233 pm, with an effective formal Ti charge of 0. The closest metal atoms to this site are three Na and three Al atoms at 250–278 pm forming an oblong octahedron. In the next four models of Table I, the Ti was substituted on the sodium sublattice along with the formation of zero, one, and two additional Na^{+1} vacancies, to result in Ti formal charges of +1, +2, and +3, respectively. The fifth model represented Na^{+1} substitution along with the removal of two additional Na^{+1} ions and an $(AlH_4)^{-1}$ group, mimicking a Ti formal charge of +2. In the remaining four models, the Ti was substituted for an Al^{+3} ion without forming an accompanying vacancy, with forming a H^{-1} vacancy, two H^{-1} vacancies, and with forming a Na^{+1} vacancy, to yield Ti formal charges of +3, +2, +1, and +4, respectively. For the proposed models with multiple possible substitution/vacancy configurations, only the configuration with vacancies in closest proximity to the Ti dopant atom was simulated. In selected cases where multiple configurations were sampled, insignificant energy differences were found.

Thermodynamical conventions were used to determine the favorability of the dopant reactions. All compound and elemental uncorrected total energies were referenced at 0 K. The enthalpy of formation, ΔH_{Form}, and the heat of substitution, ΔH_{Subst}, of the doped compounds were referenced to energies of the stoichiometric equivalents of the constituent atoms in their standard state. The latter enthalpy determines the favorability of the dopant exchange with a lattice ion and the removal of additional lattice ions for vacancy formation,

$$\Delta H_{Form}(Na_{4-k}Al_{4-l}TiH_{16-m}) = \left[E(Na_{4-k}Al_{4-l}TiH_{16-m}) - \left(E(Ti) + (4-k)E(Na) + (4-l)E(Al) + \frac{(16-m)}{2}E(H_2) \right) \right] \Big/ N_{atom}, \quad (1)$$

$$\Delta H_{Subst}(Na_{4-k}Al_{4-l}TiH_{16-m}) = \left[\left(E(Na_{4-k}Al_{4-l}TiH_{16-m}) + kE(Na) + lE(Al) + \frac{m}{2}E(H_2) - E(Na_4Al_4H_{16}) - E(Ti) \right) \right] \Big/ N_{atom}, \quad (2)$$

where $E(\mathrm{Al})$ is the uncorrected total free energy of bulk Al as calculated by VASP, etc. The indices k, l, and m refer to the number of replaced Na, Al, and H atoms, respectively. All enthalpies are reported in kJ/mol divided by the number of atoms N_{atom} (kJ/mol atom) in the substituted periodic cell.

The conditions of both a negative (exothermic) ΔH_{Form} and a negative $\Delta H_{\mathrm{Subst}}$ are together indicative of a thermodynamically stable substitution reaction. If the doped compound has a negative (exothermic) ΔH_{Form} and a positive (endothermic) $\Delta H_{\mathrm{Subst}}$, there is a small negative thermodynamic driving force for its formation, and it is metastable with respect to disproportionating to the undoped state and the pure dopant phase. The more endothermic the doping reaction, the more energy (e.g., via ball-milling) would be required for initial dopant substitution on the bulk lattice and the greater the driving force for its dissociation. A more definitive thermodynamic stability analysis (which is beyond the scope of this study) would require predicted or measured data on the Gibbs free energies of formation as a function of temperature for all possible phases, including the initial Ti additive chemistry. The Gibbs free energy minimization of the stoichiometric mixture would then be used to identify the most stable phases and reaction by-products. Metastable doped compositions are very common in nanoscale catalysts precipitated from solution, which are deployed at low enough temperatures to kinetically hinder dopant phase separation.

All of the proposed models in Table I yielded endothermic $\Delta H_{\mathrm{Subst}}$, signifying that 25% Ti substitution is metastable in all cases. Overall the results show that for any dopant/vacancy combination, models with Ti substitution on the Al sublattice yielded a more exothermic ΔH_{Form} and less endothermic $\Delta H_{\mathrm{Subst}}$ values, compared to the models with Ti substitution on the Na sublattice. Thus substitution of Ti for Al, which is closer in ionic radius and formal valence, is more feasible than Ti substitution for a larger, monovalent Na ion. The most favorable model had Ti substituted for Al and no vacancy formation, followed by the model with Ti substitution for Al and one H vacancy formed. The crystal structures of these two relaxed models are shown in Fig. 1. The effective oxidation of the substituted Ti ion by creation of Na vacancies, whether the Ti was substituted on the Na or Al sublattice, was energetically unfavorable. The enthalpy differences between the models may seem small, but it must be kept in mind that the enthalpies are reported per atom. This means that the actual enthalpy differences between competing models are at least 5 kJ/mol per unit cell, and for most of the cases it is in the order of 100 kJ/mol per unit cell. This is significant even when considering the inherent uncertainty of the GGA used.

The significant local changes in symmetry imparted by the Ti dopant atoms were manifested in the cell parameters and structural stabilities. The dopant atom broke the tetragonal $NaAlH_4$ symmetry, enabling monoclinic and triclinic cell distortions during the full minimization of the 25 mol % Ti models. These distortions were 10^{-5} degrees or smaller in magnitude in most models, but were notable in the four models of Table I with $\gamma \neq 90$. (γ was distorted in all the models with significant deviation from tetragonal symmetry.) The models with Ti substituted for Na and accompanying vacancies, all exhibited more dramatic a lattice parameter reductions and more variable c lattice parameter changes, compared to the models with Ti substituted for Al. The doped model stabilities can be rationalized in terms of changes in ionic complexation. When substituted for Al as in the $Na_4(TiH_4)(AlH_4)_3$ model [Fig. 1(b)], the Ti complexed symmetrically in 183 pm long bonds with eight H atoms in a stellated tetrahedron (stella octangula, constructed by two tetrahedra, one rotated 180° with respect to the other). This complex was formed by the sharing of the (Ti)-H atoms and four nearest-neighbor H atoms, one from each of the four adjacent AlH_4 complexes. Each adjacent Al-H complex was octahedrally coordinated with six H atoms in variable 166–182 pm long bonds. The result was a stabilizing [100] direction superlattice of stellated tetrahedra TiH_8 complexes sharing edges with four adjacent octahedral AlH_6 complexes. The formation of a H vacancy in the corresponding triclinic-distorted $Na_4(TiH_3)(AlH_4)_3$ model [Fig. 1(a)] changed the Ti-H coordination to seven, reduced the symmetry of Ti-H bond distances and complexation with the adjacent Al-H complexes. All of these changes were accommodated exothermically compared to the former fully hydrogenated model. Ti also became eight-coordinated with H, but formed longer, weaker 191 pm bonds when substituted for the Na counter-ion in the $NaTi(AlH_4)_4$ structure. This TiH_8 complex formed by disrupting the symmetry of the adjacent Al-H complexes, and sharing of H only occurred through the apexes of the adjacent AlH_4 tetrahedra. Thus, the stabilizing supercomplex formation was not fully achieved when Ti was substituted for Na.

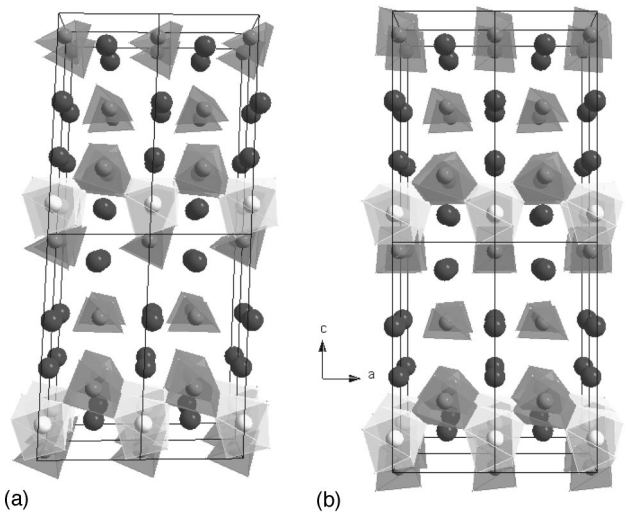

FIG. 1. The two most stable models of 25% Ti replacements in the bulk, replacing both an Al atom and a H atom (a) and replacing one Al atom (b). The dark polyhedra are AlH_n complexes, while the light polyhedra are TiH_7 complexes in (a) and TiH_8 complexes in (b). The darkest balls are Na atoms.

The simulation of selected Ti substitution configurations at a more realistic doping level of 6.25 mol %, stoichiometrically required the use of a 96 atom $2\times2\times1$ $16(NaAlH_4)$ supercell constructed from the conventional tetragonal $I4_1/a$ $4(NaAlH_4)$ cell. The six most favorable 25 mol % Ti substitution scenarios were simulated at the 6.25 mol %

TABLE II. The different models for adding 6.25% Ti to the bulk $NaAlH_4$ crystal structure. The models and formal charge of Ti follow Table I. The enthalpies of formation ΔH_{Form} and substitution $\Delta H_{\mathrm{Subst}}$ are defined in Eqs. (1) and (2), and are measured in kJ/mol atom. The lattice constants have been normalized to those of the conventional unit cell.

Substituted atoms	ΔH_{Form} (kJ/mol atom)	$\Delta H_{\mathrm{Subst}}$ (kJ/mol atom)	a_{latt} (pm)	c_{latt} (pm)	α (deg)
None	−17.6		500	1111	90.0
Interst.	−15.5	1.9	493	1106	89.9
Na	−14.6	3.0	494	1097	90.0
Al	−16.1	1.5	501	1093	90.0
Al+H	−16.0	1.8	497	1107	89.8
$Al+H_2$	−15.3	2.7	499	1107	89.6
Al+Na	−14.9	2.7	497	1103	88.1

level, listed in Table II. The relaxed model results, summarized in Table II, closely followed the 25 mol % Ti model trends. In all cases, the substitution of Ti in the $NaAlH_4$ structure yielded negative ΔH_{Form} values, but were metastable relative to the undoped structure and required energy input for the substitution to occur. The substitution of Ti for a single Al vacancy was the most favorable scenario, and again the results show more exothermic ΔH_{Form} and less endothermic $\Delta H_{\mathrm{Subst}}$ when Ti is substituted for Al than when it is substituted for Na. The predicted changes in the Ti bond distance and coordination with H were not as significant at the lower 6.25 mol % substitution compared to the 25 mol % models. When Ti was substituted for Al, eight H formed two coordination spheres around Ti. In the first sphere, four H were bonded to Ti at a distance of 181 pm, farther than the 164 pm Al-H distance in undoped $NaAlH_4$. The second sphere of four nearest neighbor H's were 234 pm away, displaced 50 pm closer than in the undoped $NaAlH_4$ by the local distortion of the four adjacent $(AlH_4)^{-1}$ complexes. At this lower substitution level, the Ti alternates with the Al atoms in both the [100] and [010] directions, forming a more dilute dopant superlattice. Thus, the symmetrical eight-coordinated stellated tetrahedron TiH_8 complex in the analogous 25 mol % Ti model, was not formed during relaxation of this supercell. Triclinic lattice distortions were simulated upon the formation of a H vacancy in the Ti complex formed on the Al sublattice. As in the analogous 25 mol % Ti model, the Ti ion become seven coordinated with H, bonding at distances from 182–206 pm away. The least favorable relaxed model of Ti substituted for the Na counterion, was coordinated to eight H atoms at a distance ranging from 197 to 227 pm. In the undoped alanate, eight H are coordinated to Na at a distance of 241 pm.

A useful analysis for comparison of our predictions to characterization data was to probe the changes in the lattice parameters for the favorable Ti substitution on the Al sublattice as a function of doping level. Additional simulations were made at the 3.125 mol % Ti dopant level, using a 192 atom $2\times2\times2$ 32($NaAlH_4$) supercell and at the 12.5% doping level, using a 48 atom supercell constructed from a $2\times2\times2$ primitive cell (in order to retain tetragonal symmetry) to augment this comparison. The substitution of one Ti ion in different size periodic models enabled the examination of different dopant levels without conducting an exhaustive study of varying configurations of relative dopant placement. The change in ΔH_{Form} and lattice parameters with doping levels ranging from 3.125 to 25.0 mol % Ti are shown in Table III and plotted in Fig. 2. The substitution enthalpy is positive for all doping levels, meaning that even down to 3 mol % Ti, doping is metastable. Extrapolating close to zero doping suggests that Ti doped Na alanate is not stable compared to pure Na alanate and elemental Ti for any doping

TABLE III. Variation of the formation enthalpy ΔH_{Form} and the substitution enthalpy $\Delta H_{\mathrm{Subst}}$ as a function of the Ti content. The enthalpies are measured in kJ/mol atom. Ti has been placed on an Al site, substituting one Al atom. The results are compared to pure $NaAlH_4$. Also shown is the number of atoms in the unit cell N_a of the different models and the lattice constants of the final relaxed lattice. The lattice constants have been normalized to the conventional unit cell. In all the models, tetragonal symmetry within the accuracy of our calculations was retained after the relaxation was finished.

Ti content (%)	N_a	ΔH_{Form} (kJ/mol atom)	$\Delta H_{\mathrm{Subst}}$ (kJ/mol atom)	a_{latt} (pm)	c_{latt} (pm)
0	24	−17.6		500	1111
3.125	192	−16.8	0.8	501	1102
6.25	96	−16.1	1.5	501	1093
12.5	48	−14.7	2.9	500	1079
25	24	−14.2	3.4	491	1103

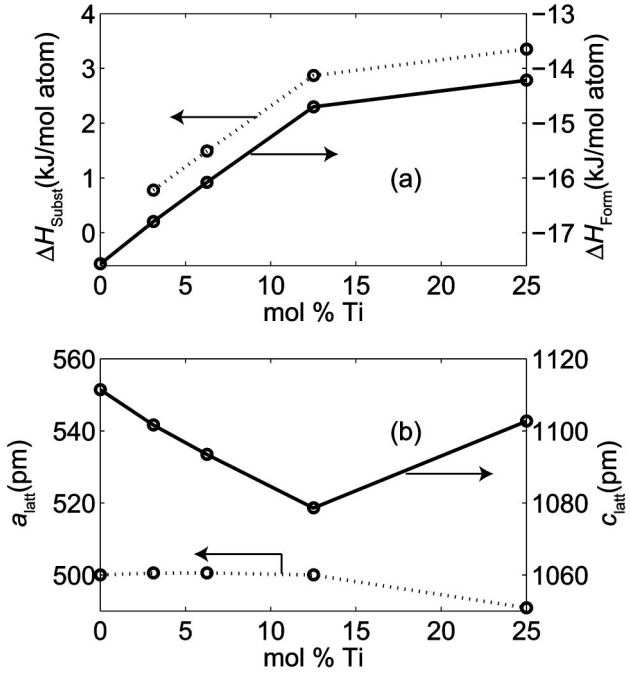

FIG. 2. Variation of the enthalpies ΔH_{Form} and $\Delta H_{\mathrm{Subst}}$ in kJ/mol atom (a) and the lattice constants in picometers (b) as functions of the Ti content in doped $NaAlH_4$.

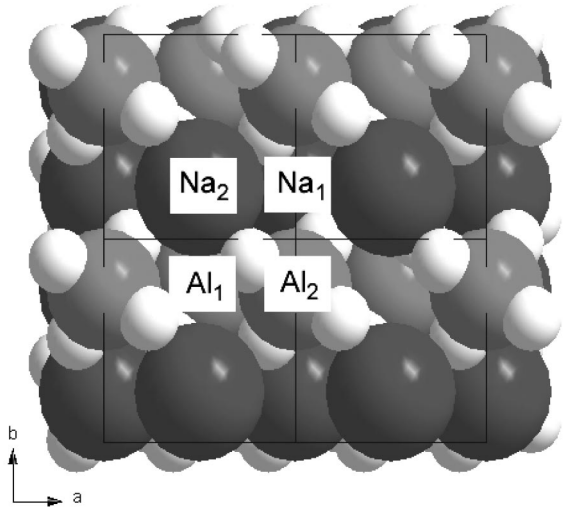

FIG. 3. The Ti interstitial adsorption and absorption sites on the $NaAlH_4$ (001) surface seen from above. The small white balls are hydrogen atoms, while the light and dark gray balls are Al and Na atoms, respectively. The Al_1 and Na_1 sites are located in the surface layer, directly above an Al and Na atom in the second layer, respectively. Similarly, the Al_2 and Na_2 sites are located in the second layer (subsurface), directly below Al and Na atoms in the surface layer. The 2×2 surface unit cell used in our calculations consists of the four conventional surface unit cells that are outlined.

level. We must bear in mind, however, that the calculations are performed using periodic supercells at 0 K. Both configurational entropy and temperature effects, particularly vibrational entropy, could possibly stabilize the doped phases. It is, however, also evident from Table III that the lattice constants change significantly when Al is replacing Ti, even when the Ti content is as low as 3.125%. Such large changes would have been seen by the accurate diffraction studies of Ref. 15, either by a change in the overall lattice constants if Ti were crystalline, or as a broadening of the peaks if Ti were distributed randomly. Since neither of these are seen, we conclude that none of our models for Ti substitution in the bulk are consistent with the experimental data available for Ti solvated in the bulk $NaAlH_4$ phase. This may either mean that these models are not stable and thus do not exist, or that the solid solution of Ti in bulk $NaAlH_4$ was not achieved in preparation of the samples being used in the above mentioned experimental studies. The latter explanation may be possible, since the samples have been doped after, and not during, synthesis.[12,15] If they had been doped at the same time as when being synthesized,[28] the doping could possibly have led to a larger probability for Ti absorption in the bulk $NaAlH_4$. Our results for the lattice constant changes are also not compatible with the only previous experimental study that showed changes in the lattice constants as doping level changed.[11]

IV. TI AS SURFACE CATALYST

Titanium additions have been shown to effectively catalyze both $NaAlH_4$ disproportionation/dehydrogenation and comproportionation/hydrogenation processes involving the redistribution and transformation of multiple phases. To probe whether titanium could play a surface-active role in the processes, we have evaluated models of titanium near-surface lattice substitution (analogous to the bulk models), interstitial absorption, and surface adsorption in 96 atom NaAlH4 (001) $2\times2\times1$ slabs. The latter models introduce Ti as a monodisperse metal-loaded heterogeneous catalyst, without replacing any of the alanate ions. Here, Ti was effectively input with a 0 formal charge; nonetheless, the added Ti could easily give charge to its surroundings to achieve a more realistic effective charge. Figure 3 shows the different possible adsorption sites that are investigated in this study. Ti was added to such interstitial sites in the same layer as the neighbor metal atoms, directly below a surface metal atom in the second layer, or 28 pm directly above a surface atom as an adsorbed species. Since the number of available H atoms for bonding is low above the surface, the adsorption models were highly unstable, and have not been included in what follows.

Table IV shows the heats of formation and the heats of substitution or interstitial adsorption (for the cases that no substrate atoms were removed) of Ti for the various slab models, relative to the similarly relaxed $NaAlH_4$ (001) slab and elemental Ti [see Eqs. (1) and (2)]. The heat of substitution for Ti substituted at different lattice layers with respect to the slab surface is shown in Fig. 4. Since there are only four layers of the slab and the bottom layer was kept fixed, we only regarded replacements in the upper three layers. We first note that exactly the same trend is seen as in the bulk. The most stable models are those substituting Ti at Al sites, with Al substitution and AlH substitution being the most stable possibilities. To replace a Na ion is less stable by more

TABLE IV. The substitution enthalpy ΔH_{Subst} of Ti at the $2\times2\times1$ (001) slab of $NaAlH_4$. When no atoms are substituted, ΔH_{Subst} is simply the negative of the adsorption energy E_{Ads}. The specified adsorption sites are shown in Fig. 3. The enthalpies are given in kJ/mol atom.

		ΔH_{Subst} (kJ/mol atom)		
Substituted atoms	Ads. site	Layer 1	Layer 2	Layer 3
Na		2.4	2.5	3.2
Al		1.5	0.7	1.3
AlH		1.1	1.1	1.7
AlH_2		3.1	2.0	3.0
	Na_1	3.9		
	Al_1	2.0		
	Al_2		2.1	
	Na_2		2.1	

than 1 kJ/mol atom, and the addition of Ti as an interstitial adsorbent is more beneficial than Na substitution without vacancy formation.

The substitution layer determined the availability of neighboring species that could complex with and stabilize the Ti dopant. In the most stable configuration, Ti substituted for Al in the second layer, the Ti ion is coordinated to eight hydrogens, four of which are gathered from neighboring AlH_4 complexes like in the analogous bulk model. In the next most stable configuration, Ti substitution for Al in the first layer accompanied by the formation of a hydrogen vacancy, the Ti atom submerged towards the second layer to interact with two adjacent AlH_4 complexes. In this relaxed

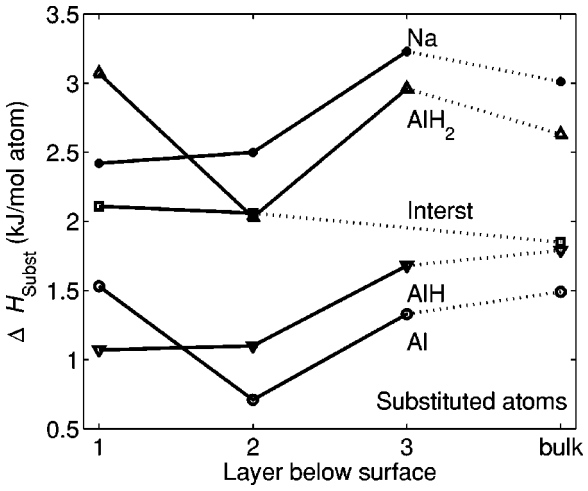

FIG. 4. The substitution enthalpy ΔH_{Subst} of Ti on a $2\times2\times1$ slab as a function of the layer in which Ti is placed—layer 1 is the surface layer, etc. The resulting Ti content is 6.25 mol %. Ti is replacing the specified atomic groups (except when Ti is adsorbed at an interstitial site and no atoms are replaced, marked by "Interst"), and the ΔH_{Subst} is calculated relative to the pure slab and the interchanging elements in their standard form [Eq. (2)]. Also shown is ΔH_{Subst} in the bulk, for comparison.

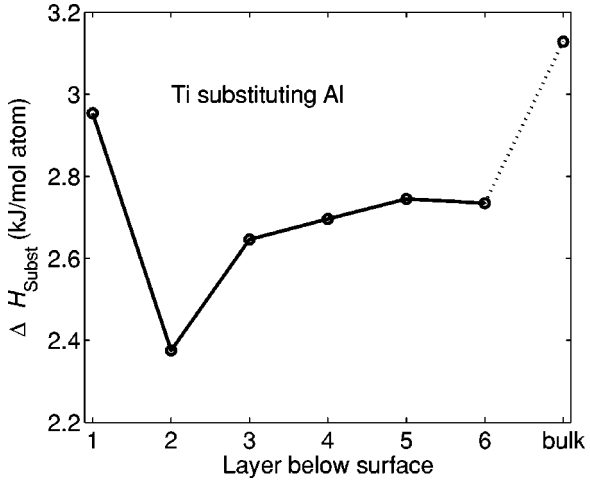

FIG. 5. The substitution enthalpy of Ti on a $1\times1\times2$ slab as a function of the layer in which Ti is placed—layer 1 is the surface layer, etc. The resulting Ti content is 12.5 mol %. Ti is replacing one Al atom, and the substitution enthalpy is calculated relative to the pure slab and Ti and Al in their standard form [Eq. (2)]. Also shown is ΔH_{Subst} in the bulk, for comparison.

slab, the Ti atom was complexed directly with seven hydrogen atoms. Thus, the removal of a hydrogen atom adjacent to the surface substituted Ti atom represents a favorable, exothermic scenario for atomic hydrogen dissociation from the $NaAlH_4$ surface. The dopant proximity to the lower coordinative environment at the slab surface enabled greater degrees of freedom in the relaxation of the doped slab structures. As expected, surface stabilization effects were less pronounced when the dopant was substituted in the third layer. It is also very interesting to note that in the most stable cases, bulk substitution is significantly less favorable than any of the slab models. This is despite the fact that the bulk models were allowed to relax cell sizes, while the slab models were not. (In both cases, the enthalpy was calculated relative to the undoped/uncatalyzed models being relaxed in the same procedure as the doped/catalyzed one.) Since the bulk models gained significantly from the cell size changes, the difference between bulk and surface substitution could be even larger than Fig. 4 implies.

Since the fourth layer was fixed in the $2\times2\times1$ (001) models, we could not be sure that the second layer being most stable is an artifact of the relatively thin model slab, since the possibility for relaxation around the replaced species may be considerably reduced when Ti is substituted in the third layer. We have therefore performed the $Al\rightarrow Ti$ substitution in a 48 atom $1\times1\times2$ slab with eight metal layers, in order to check whether our conclusions are affected by the layer thickness. Using the same procedure as above, only now with a $1\times1\times2$ slab, we achieved the substitution enthalpy as shown in Fig. 5. Exactly the same trend is seen as in Fig. 4; the surface site is the least stable of the slab sites, while the subsurface site is the most stable. Bulk substitution is significantly less stable in this case as well.

We have now calculated ΔH_{Subst} on two slabs with 12.5 and 6.25 mol % Ti replacing Al in the second (subsurface) layer. If ΔH_{Subst} is extrapolated linearly from these two

points down to very low Ti content, we find that $\Delta H_{\mathrm{Subst}}$ becomes negative when the Ti filling fraction is below around 3.5 mol % Ti. Substitution of Ti approaches -1 kJ/mol atom at the very lowest fractions. Thus, if this extrapolation is valid, we have identified stable substitution of Ti in the lattice subsurface. Caution should be taken, however, since the distribution of substituted Ti is different than in the bulk models: Ti has four nearest Ti neighbors at only 500 pm in the $1\times1\times2$ slab model with 12.5 mol %, while the shortest distance between Ti atoms is 707 pm in the $2\times2\times2$ bulk primitive cell with 6.25 mol % Ti. Calculating Ti adsorption on the $2\times2\times2$ slab model with 3.125 mol % Ti would have resolved this, but this model is currently too large. If the surface density of Ti is important, rather than the resulting bulk content from Ti adsorption, we should extrapolate $\Delta H_{\mathrm{Subst}}$ as a function of the Ti surface density, for instance defined as the number of substituted Ti atoms per unit surface area. In that case we obtain unstable adsorption even at the smallest surface densities. We conclude that surface adsorption is more stable than bulk absorption, but still probably unstable or metastable for all concentrations.

V. DISCUSSION

Our methodology served to evaluate the influence of Ti substitution on the stability of the $NaAlH_4$ lattice, in order to locally assess whether such substitution is thermodynamically possible in the ground state. To accomplish this in the bulk doped models, we invoked full minimization of all available degrees of freedom allowed by the symmetry of the starting doped model. In doing so, we set the stage for the best opportunity for the dopant molecule to be accommodated within the lattice, at the risk of over-relaxing the atomic configurations. Commonly in dopant studies, only atoms in a selected radius around the dopant are allowed to relax. However, this would result in less favorable configurations. Indeed, we attempted to eliminate triclinic distortions in lower symmetry doped models by enforcing tetragonal symmetry. A separate series of calculations were made enforcing tetragonal symmetry by iteratively minimizing the ionic positions and the cell volume. A further modification of this procedure was conducted, by minimizing the volume of a range of models with systematically varying c/a ratios. These tetragonal relaxed structures by either of these methods were not as low in energy as the fully relaxed models, and were discarded from that reason. Our largest models are also performed at realistic doping levels, making full relaxation the most relevant procedure.

Our methodology of surveying limited configurations for varying dopant substitution and dopant levels did not provide the direct opportunity for assessing higher order configurational interactions. Thus, our modeling results must not be construed to comprehensively represent random dopant substitution within the bulk or surface and the possible stabilizing effects of a high configurational entropy. Thermodynamically, the ideal configurational entropy is given as

$$S_{\mathrm{Config}} = R\sum_s a_s \sum_i x_i \ln x_i, \tag{3}$$

where R is the ideal gas constant, a_s are the fraction of all sites belonging to the s sublattice, and x_i are the site fractions on the s sublattice.[29]

For example, with 6.25% dopant substituted only on one sublattice without vacancy formation, the ideal configurational entropy times temperature at 298 K would be $S_{\mathrm{Config}}\times T=-0.0965$ kJ/mol atom. This would not provide enough stabilization of the doped lattice relative to the undoped phase over the relevant temperature range. A systematic series of models evaluating dopant-dopant and dopant-lattice interactions in the context of Monte Carlo or cluster variation methodology, would be required to theoretically assess additional nonideal associative or repulsive configurational interactions at finite temperatures. Somewhat more accessible would be to assess the solubility limit dopant concentration at a given temperature, using the calculated formation energies in combination with standard thermodynamics.[30] This has not been addressed here, but we note the possibility of finite population of metastable sites.

Other configurational contributions could be Ti association of lattice defects, either introduced by Ti inclusion or preparation processing, like for instance ball milling. This should have been observed as a change in line broadening in the diffraction studies of doped alanate. The lack of reported difference in broadening between pure and Ti-enhanced sodium alanates does not point to Ti-induced defects.[15] This has thus not been considered further in this work.

Our study also did not take vibrational contributions into account, due to the computational demand of conducting vibrational simulation methods on large supercells. Nevertheless, the systematic omission of the zero point energy on all models should not have a significant impact on assessing relative stability at the ground state, though vibrational contributions at elevated temperatures may vary significantly with the symmetry and constitution of the doped lattice.

In our substituted slab models, we changed to invoking the undoped slab parameters and only allowing relaxation of the ions. This approach enabled us to evaluate local substitutional effects at the surface, without predisposing the models with dopant-induced bulk lattice parameters. The latter approach would have required an initial relaxation of the doped-bulk state, cleavage of the relaxed bulk model at a selected lattice plane to position the dopant atom relative to the surface, and finally relaxation of the cleaved slab with the bottom layer fixed at bulk parameters. We followed this latter methodology with a series of models of Ti substituted for Al at different layers relative to the surface. These relaxed models were not as low in energy as those relaxed with our selected procedure, and thus discarded.

Our calculations have revealed that at the ground state, the undoped $NaAlH_4$ phase has a more favorable heat of formation than any of the Ti-doped $NaAlH_4$ models, with respect to the constituting elements in their standard states. The smallest difference between undoped $NaAlH_4$ and 6.25% Ti in $NaAlH_4$ is for the slab model with Ti substituted immediately below the surface (layer 2) on the Al sublattice. Here, the difference in heats of formation is 0.71 kJ/mol atom. This energy difference is large enough to exclude the possibility of an ordered phase with several percent Ti substituted in the bulk lattice. Still, metastable dopant incorporation induced with high energy ball-milling is entirely plausible. However, the kinetic effect of the additive lasts for at least 100 hydrogenation/dehydrogenation cycles which do

not involve ball-milling.[15] This is a strong indication that bulk substitution does not provide the explanation of the enhanced kinetics.

Alternatively, the Ti included in the lattice near or at the surface of $NaAlH_4$ may be regarded as a heterogeneous catalyst. The classical role of Ti would then be to enhance dissociation of H_2 upon hydrogenation and association of H_2 upon dehydrogenation. Another possible catalyticlike role of Ti at the surface is to enhance internal kinetics. We have calculated the barriers for hydrogen mobility at and near the surface, and found that the inclusion of Ti strongly increases the mobility of the hydrogen species.[31] The full explanation of the catalytic role of the added Ti could of course involve both these mechanisms.

It is well-known that the most stable product containing Ti in the Na-Ti-Al-H system is the $TiAl_3$ $D0_{22}$ intermetallic compound, as seen in the dehydrogenated Ti-enhanced $NaAlH_4$.[17] Regardless of where the added Ti atoms are situated, the tendency to form $TiAl_3$ or other Ti-Al intermetallic phases upon dehydrogenation will serve to further destabilize the Ti-activated sodium alanate phase. This is because the increased reaction enthalpy from the formation of more stable Ti-Al reaction products will effectively increase the dissociation pressure, as described by the van't-Hoff relationship. In addition, since the formation of Ti-Al phases are more exothermic or favorable, the corresponding decrease in the activation barrier could serve to kinetically enhance the disproportionation reaction. This is interpreted from the well-known Evans-Polanyi relationship, which shows a strong correlation between increasing reaction rates, decreasing activation barriers, and decreasing reaction enthalpies for many systems.[32]

We have, together with the experimental evidence, excluded bulk ordered substitution at concentrations in the order of a few percent or higher. There is a possibility that Ti is present amorphously at the Al sublattice, preferentially near the surface. The most plausible scenario is, in our opinion, that Ti is present both as a surface substituted species and in distributed Ti-Al intermetallic phases. But this is only the starting point for the dehydrogenation process. In order to understand fully the role of Ti as additive, we need to investigate possible phases and scenarios also for the Ti-enhanced Na_3AlH_6 phase and for the fully dehydrogenated mixture of NaH, Al, and Ti bearing phases. These mechanisms are important to study, because the rehydrogenation, particularly of the Na_3AlH_6 to $NaAlH_4$ phase, is the critical step in the cycling performance.

Equally important would be to investigate in detail kinetic models for the phase transformations. It is already known that there is a clear evolution of the cycling behavior when the doped samples are cycled several times,[15] and this is most probably related to the development of different stable and metastable phases. It could be both due to the disappearance of metastable inclusion of Ti enforced by the ball-milling, or by decomposition to a stable binary Ti-Al phase.

VI. CONCLUSIONS

Accurate density functional calculations have been used to clarify the location of Ti in doped/catalyzed $NaAlH_4$, based on the assumption that Ti is either replacing one or more atoms in the host lattice, either in the bulk or at the surface, or that Ti occupies interstitial adsorption sites at the surface. It has been revealed that the least unfavorable arrangement compared to pure $NaAlH_4$ and the pure metals is Ti replacing Al in the lattice. It has also been found that the least unfavorable arrangement is with Ti placed in the second metal layer from the surface, since this both gives the possibility to relax the structure significantly and to provide enough hydrogen atoms around the Ti atom to make the preferred coordination possible.

Such substitution is found to be thermodynamically metastable, and either configurational and/or vibrational entropy contributions are needed to make it feasible. Also, the calculated changes in the lattice parameters are significantly larger for these bulk dopant models than what has been observed experimentally. The model that points itself out as the most probable for explaining the kinetic enhancement of adding Ti, is thus random Ti substitution at or near the $NaAlH_4$ surfaces and interfaces. This is most probably accompanied by the formation of binary amorphous TiAl intermetallic phases.

ACKNOWLEDGMENTS

Stimulating discussions with Hendrik Brinks and Bjørn Hauback are gratefully acknowledged by O.M.L., who has received financial support and computing time from the Norwegian Research Council. S.M.O. acknowledges important technical interactions with Dr. D. L. Anton and the support of US DoE under Contract No. DE-FC04-02AL67610 for the duration of this work.

[1] B. Bogdanovic and M. Schwickardi, J. Alloys Compd. **253**, 1 (1997).
[2] C. M. Jensen and K. J. Gross, Appl. Phys. A: Mater. Sci. Process. **A72**, 213 (2001).
[3] K. J. Gross, G. J. Thomas, and C. M. Jensen, J. Alloys Compd. **330–332**, 683 (2002).
[4] M. Fichtner, J. Engel, O. Fuhr, O. Kircher, and O. Rubner, Mater. Sci. Eng., B **108**, 42 (2004).
[5] D. L. Anton, J. Alloys Compd. **356–357**, 400 (2003).
[6] B. Bogdanovic, R. A. Brand, A. Marjanovic, M. Schwickardi, and J. Tolle, J. Alloys Compd. **302**, 36 (2000).
[7] B. Bogdanovic, M. Felderhoff, S. Kaskel, A. Pommerin, K. Schlichte, and F. Schüth, Adv. Mater. (Weinheim, Ger.) **15**, 1012 (2003).
[8] M. Fichtner, O. Fuhr, O. Kircher, and J. Rothe, Nanotechnology **14**, 778 (2003).
[9] K. J. Gross, S. Guthrie, S. Takara, and G. J. Thomas, J. Alloys Compd. **297**, 270 (2000).

[10] G. J. Thomas, K. J. Gross, N. Y. C. Yang, and C. M. Jensen, J. Alloys Compd. **330–332**, 702 (2002).
[11] D. Sun, T. Kiyobayashi, H. T. Takeshita, N. Kuriyama, and C. M. Jensen, J. Alloys Compd. **337**, L8 (2002).
[12] B. Bogdanovic, M. Felderhoff, M. Germann, M. Härtel, A. Pommerin, F. Schüth, C. Weidenthaler, and B. Zibrowius, J. Alloys Compd. **350**, 246 (2003).
[13] J. Iniguez, T. Yildirim, T. J. Udovic, E. H. Majzoub, M. Sulic, and C. M. Jensen, Phys. Rev. B **70**, 060101(R) (2004).
[14] J. Graetz, J. J. Reilly, J. Johnson, A. Y. Ignatov, and T. Y. Tyson, Appl. Phys. Lett. **85**, 500 (2004).
[15] H. W. Brinks, C. M. Jensen, S. S. Srinivasan, B. C. Hauback, D. Blanchard, and K. Murphy, J. Alloys Compd. **376**, 215 (2004).
[16] V. Ozolins, E. H. Majzoub, and T. J. Udovic, J. Alloys Compd. **375**, 1 (2004).
[17] E. H. Majzoub and K. J. Gross, J. Alloys Compd. **356–357**, 363 (2003).
[18] V. P. Balema, J. W. Wiench, K. W. Dennis, M. Pruski, and V. K. Pecharsky, J. Alloys Compd. **329**, 108 (2001).
[19] R. A. Zidan, S. Takara, A. G. Hee, and C. M. Jensen, J. Alloys Compd. **285**, 119 (1999).
[20] G. Kresse and J. Hafner, Phys. Rev. B **47**, 558 (1993).
[21] G. Kresse and J. Furthmüller, Phys. Rev. B **54**, 11 169 (1996).
[22] J. P. Perdew, J. A. Chevary, S. H. Vosko, K. A. Jackson, M. R. Pederson, D. J. Singh, and C. Fiolhais, Phys. Rev. B **46**, 6671 (1992).
[23] G. Kresse and D. Joubert, Phys. Rev. B **59**, 1758 (1999).
[24] MedeA: Materials Exploration and Design Analysis, Copyright 1998–2003, Materials Design, Inc.
[25] S. M. Opalka and D. L. Anton, J. Alloys Compd. **356–357**, 486 (2003).
[26] B. C. Hauback, H. W. Brinks, C. M. Jensen, K. Murphy, and A. J. Maeland, J. Alloys Compd. **358**, 142 (2003).
[27] T. Frankcombe and O. M. Løvvik, in preparation.
[28] B. Bogdanovic and M. Schwickardi, Appl. Phys. A: Mater. Sci. Process. **A72**, 221 (2001).
[29] M. Hillert, *Phase Equilibria, Phase Diagrams and Phase Tranformations. Their Thermodynamic Basis* (Cambridge University Press, Cambridge, 1998).
[30] J. M. Sullivan and S. C. Erwin, Phys. Rev. B **67**, 144415 (2003).
[31] S. M. Opalka and O. M. Løvvik (unpublished).
[32] R. I. Masel, *Principles of Adsorption and Reaction on Solid Surfaces* (Wiley, New York, 1996).